Journal of Alloys and Compounds 608 (2014) 73–78

Contents lists available at ScienceDirect

Journal of Alloys and Compounds

journal homepage: www.elsevier.com/locate/jalcom

Sr_2CeO_4: Electronic and structural properties

Leonardo A. Rocha [a], Marco A. Schiavon [a], Clebio S. Nascimento Jr. [b], Luciana Guimarães [b], Márcio S. Góes [c], Ana M. Pires [d], Carlos O. Paiva-Santos [e], Osvaldo A. Serra [f], Marco A. Cebim [e], Marian R. Davolos [e], Jefferson L. Ferrari [a,*]

[a] Grupo de Pesquisa em Química de Materiais – (GPQM), Departamento de Ciências Naturais, Universidade Federal de São João del-Rei, Campus Dom Bosco, Praça Dom Helvécio, 74, 36301-160 São João del-Rei, MG, Brazil
[b] Laboratório de Química Teórica e Computacional – (LQTC), Departamento de Ciências Naturais, Universidade Federal de São João del-Rei, Campus Dom Bosco, Praça Dom Helvécio, 74, 36301-160 São João del-Rei, MG, Brazil
[c] Universidade Federal da Integração Latino-Americana (UNILA), Av. Tancredo Neves, 6731 – Bloco 4, Cx P. 2044, CEP: 85867-970 Foz do Iguaçu, PR, Brazil
[d] Faculdade de Ciências e Tecnologia, UNESP Univ. Estadual Paulista, 19060-900 Presidente Prudente, SP, Brazil.
[e] Instituto de Química, Unesp Univ. Estadual Paulista, P.O. Box 355, 14800-970 Araraquara, SP, Brazil.
[f] Departamento de Química, Faculdade de Filosofia, Ciências e Letras de Ribeirão Preto, Universidade de São Paulo, 14040-901 Ribeirão Preto, SP, Brazil

ARTICLE INFO

Article history:
Received 22 January 2014
Received in revised form 14 April 2014
Accepted 15 April 2014
Available online 24 April 2014

Keywords:
Photoluminescence
Rietveld
Cerate
X-ray
Rare earths

ABSTRACT

This work presents on the preparation and photoluminescent properties of Sr_2CeO_4 obtained from the heat treatment of Ce(III)-doped strontium oxalate (10, 25 and 33 mol%). The oxalate precursors were heat treated at 1100 °C for 12 h. The structure of this photoluminescent material was evaluated by the Rietveld method. The route used in this work to prepare the materials showed to be viable when compared to other synthesis reported in the literature. The Sr_2CeO_4 material showed a broad and intense band emission with a maximum around 485 nm. The quantitative phase analysis showed that the Sr_2CeO_4 photoluminescent phase is the majority one compared to the impurity phases of $SrCeO_3$ and $SrCO_3$. From all results it was possible to verify a complete elimination of the CeO_2 phase for the sample obtained from the heat treatment of oxalate precursor containing 33 mol% of cerium(III). The material showed excellent properties for possible candidate as scintillator materials, and in the improvement of efficiency of solar cells when excited in the UV–vis region. The CIE chromaticity diagram it is also reported in this work.

1. Introduction

In the last several decades, research has been focused on oxide-based photoluminescent materials due to their commercial applications in color television, fluorescent tube, X-ray phosphors, and scintillators [1–3]. To avoid degradation when exposed under high energy radiation, theses oxide systems need to show adequate mechanical resistance and chemical stability. Among the different phosphors that have the above-cited properties and also exhibit blue emission, only a few are available as blue photoluminescent materials for devices.

In the 90s, a new rare-earth-based photoluminescent material with chemical formula Sr_2CeO_4 showing an emission peak around 485 nm was reported by Danielson et al. [4]. The authors synthesized this material by a combinatorial chemical procedure, and successfully identified the structure through structural analysis by X-ray diffraction (XRD) and the Rietveld method [5] for refinement of the structure. Since then, many studies have been reported in the literature describing its importance and contribution as a blue photoluminescent material [6–9]. In parallel, some authors have published information on the application of Sr_2CeO_4 as a host of other rare earths yielding excellent optical features [10] in different regions of the electromagnetic spectrum.

In accordance with many papers reported in the literature, the photoluminescence of Sr_2CeO_4 is a consequence of the energy transfer between O^{2-} and Ce(IV) localized in one-dimensional chains of the edge-sharing CeO_6 octahedron [11–15]. Also, it has been proven that the photoluminescence depends directly on the size and shape of particles [16–18]. Among the several methods to prepare the photoluminescent Sr_2CeO_4, the thermal decomposition of acetates, oxalates or carbonates, microwave calcinations, pulsed laser deposition and Pechini method are examples mostly cited in the literature [11,19–25]. However, the presence of secondary phases, such as $SrCeO_3$, $SrCO_3$ and CeO_2 [26], along with the photoluminescent Sr_2CeO_4 are observed regardless of the preparation route. In this sense, systematic studies considering the amounts of phases present together with the phosphor after

* Corresponding author. Tel./fax: +55 32 3379 2483.
E-mail addresses: ferrari@ufsj.edu.br, jeffersonferrari@gmail.com (J.L. Ferrari).

http://dx.doi.org/10.1016/j.jallcom.2014.04.091
0925-8388/

its synthesis should be evaluated in order to facilitate the understanding of the mechanisms to obtain the Sr_2CeO_4 phase with optimized photoluminescent properties. Therefore, the aim of this work is to report on the preparation of the photoluminescent material Sr_2CeO_4 starting from 10, 25 to 33 mol% of Ce(III)-doped strontium oxalate. The synthetic route chosen in this work was previously reported as an alternative way for obtaining the photoluminescent material with properties suitable for various applications. Moreover, the methodology used here is one of the most common for bulk materials production because it is simple, low cost, low temperature, and also allows the control of the solution homogeneity [25,27]. In addition, the spectroscopy properties of the Sr_2CeO_4 samples prepared from the oxalate precursors were investigated and correlated with the structural refinement that was made based on the Rietveld method [5].

2. Material and methods

The synthesis used here has been described in prior work [27]. However, the percentage of Ce(III) in strontium oxalate used as precursor were 10, 25, and 33 mol%. The precursors were prepared from the mixture of the metal chloride solutions, $SrCl_2{\cdot}6H_2O$ (VETEC, 99.99% purity), and $CeCl_3{\cdot}7H_2O$ (ALDRICH, 99.999% purity), with $(NH_4)_2C_2O_4{\cdot}H_2O$ (REAGEM, 99% purity) solution, and heated at 80 °C (pH≅1). The Ce(III) concentrations reported in this work were used to obtain material with a greater quantity of Sr_2CeO_4 luminescent phase. After the adjustment of the pH to ~4, the temperature was increased to 80 °C, and the solution was kept under ultrasonic stirring for 1 h. Then, it was left to rest for 4 h prior to posterior filtration and dried under reduced pressure in a desiccator with silica gel and calcium chloride. These precursors were heat treated at 1100 °C in a horizontal oven with heating rate of 20 °C/min, for 12 h in a static air atmosphere to obtain the final product. All products of thermal decomposition of the precursors were analyzed by X-ray diffraction (XRD) using a D5000 SIEMENS® diffractometer, using Cu Kα radiation ($\lambda_{K\alpha1}$ = 1.5405 Å, $\lambda_{K\alpha2}$ = 1.5443 Å), in the 2θ range between 14° and 70°, step of 0.02 (2θ) with 1.0 s per point. The product of thermal decomposition of the precursor with 33 mol% of Ce^{3+} was also analyzed by XRD, using a Rigaku® RINT2000 diffractometer (42 kV × 120 mA) using Cu Kα radiation ($\lambda_{K\alpha1}$ = 1.5405 Å, $\lambda_{K\alpha2}$ = 1.5443 Å, $I_{K\alpha1}/I_{K\alpha2}$ = 0.5), in the 2θ range between 15° and 120°, step 0.02° (2θ) with 2.0 s/step, using a divergence slit = 0.5 mm, and receiving slit = 0.3 mm. The Rietveld refinements [5] were calculated using the program package General Structure Analysis System (GSAS) program of Larson & Von Dreele [28], and graphical user interface EXPGUI [29]. Peak profile functions were modeled using a convolution of the Thompson–Cox–Hastings pseudo-Voigt function [30] with the asymmetry function described by Finger et al. [31], which accounts for the asymmetry due to axial divergence. Based on the results of Rietveld refinement structure we performed a semi empirical Sparkle/PM7 solid state calculation in order to obtain the band gap energy through the HOMO/LUMO energy difference. The calculation was carried out using the MOPAC2012 computational package. Diffuse reflectance spectrum was employed to the S33 material for calculation of the experimental band gap using the Kubelka–Munk was submitted. All products displayed emission under UV excitation (λ_{exc} = 275 nm), and were investigated by photoluminescence spectroscopy in the visible region (in the range between 375 and 700 nm) using a Fluorolog SPEX F212I fluorescence spectrofluorimeter equipped with an R928 Hammamatsu photomultiplier and a 450 W Xe lamp). The emission spectrum of the material showing the more intense emission was used to build the CIE chromaticity diagram 1931. It is important to report that the precursor used to obtain better intensity of photoluminescence of the final product, was that containing 33 mol% of Ce(III). In order to obtain scintillation properties, the X-ray excited optical luminescence (XEOL) spectra were obtained in a homemade system [32]. The powders were excited with radiation of copper X-ray tube (operating at 35 kV and 20 mA) and the luminescence signal was collected in front-face mode by optical fiber coupled to Shamrock SR-303i spectrometer and detected in a CCD camera Newton USB DU940-BV with 2048 × 512 pixels, both from Andor Technology.

3. Results and discussion

In order to facilitate the presentation of the results, the samples obtained from the heat treatment of the precursor containing 10, 25 and 33 mol% of Ce(III) were labeled as S10, S25 and S33, respectively. In previous works reported by Moosath et al. [33] and Ferrari et al. [25], the Ce(III) ions undergo a thermal oxidation during the thermal treatment of the oxalate precursor at around 343 °C resulting in Ce(IV) ions. Consequently, after the thermal oxidation during the reaction, the reagents available led to the formation of the photoluminescent Sr_2CeO_4 phase.

The emission spectra (λ_{exc} = 275 nm) recorded for the photoluminescent samples are depicted in Fig. 1, where a large emission band centered at 480 nm is observed, independent from the precursor used in the preparation of the samples. In accordance with Lu et al. [11], the emission band is assigned to a metal-to-ligand transition between Ce(IV) → O^{2-}, in the case of the photoluminescent Sr_2CeO_4, where two different O^{2-} positions exist in the structure of the material (equatorial and terminal positions).

In order to obtain more detail about the nature of the emission, each emission spectrum was deconvoluted in two bands that are assigned to each Ce(IV) → O^{2-} charge transfer transition [17]

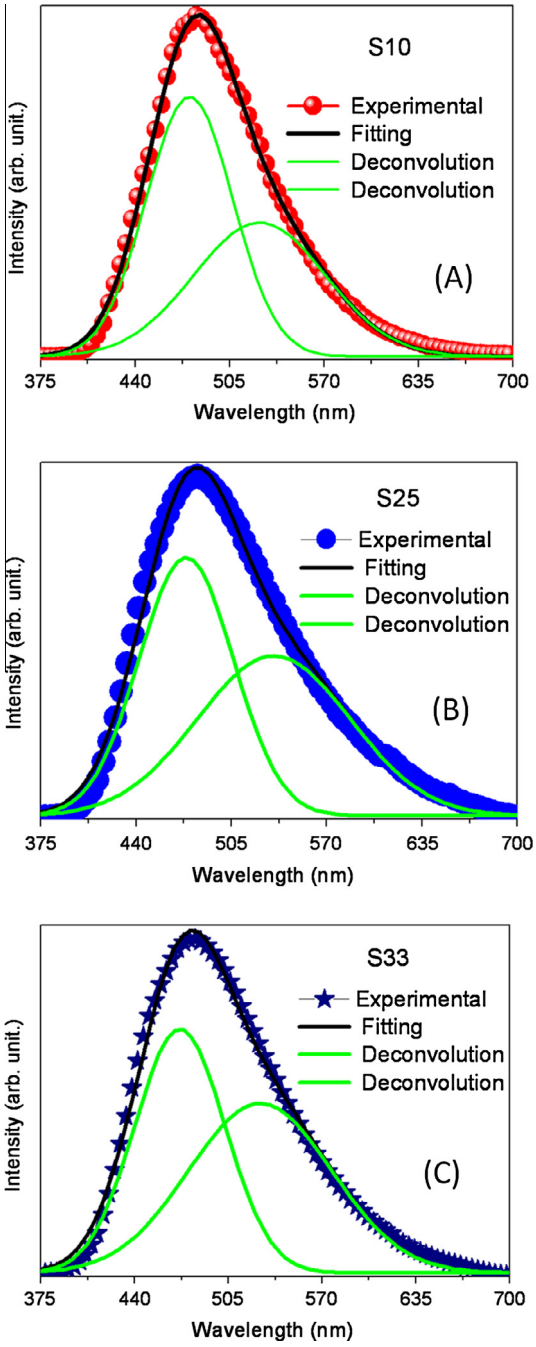

Fig. 1. Emission photoluminescence spectra deconvoluted of the (A) S10, (B) S25 and (C) S33 samples.

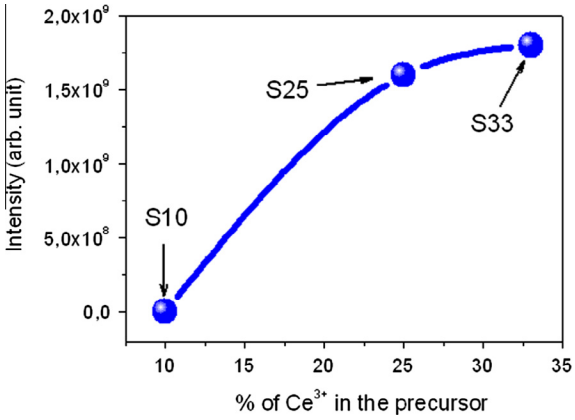

Fig. 2. Relative intensity based on the photoluminescence emission spectra of the S10, S25 and S33 samples.

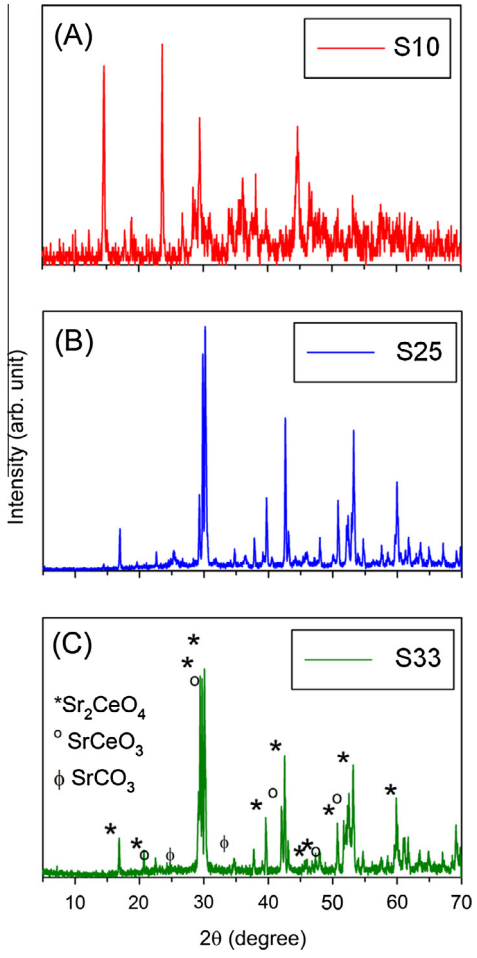

Fig. 3. XRD patterns of (A) S10, (B) S25 and (C) S33 samples.

related to the different oxygen positions in the Sr_2CeO_4 structure. Lu et al. [11] established that the energy levels of terminal and equatorial metal-to-ligand excited states were 2.58 and 2.32 eV above the ground state, respectively, for the system reported. In the case of the present work, the energies were estimated as being around 2.59 and 2.36 eV for sample S10, 2.61 and 2.31 eV for sample S25, and 2.62 and 2.34 eV for sample S33, all in agreement with the data reported in the literature [11]. The variation of the energy levels estimated for the different samples may be related to the

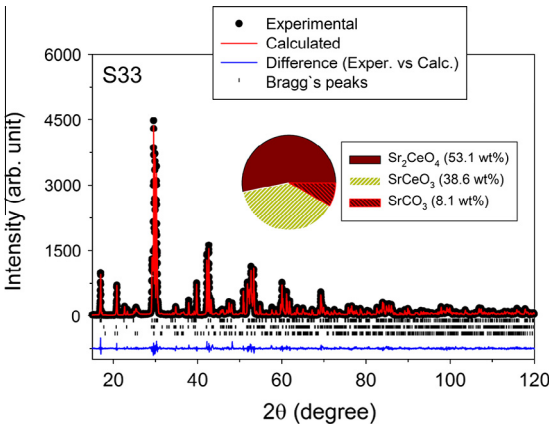

Fig. 4. Rietveld plot of the S33 sample. The small vertical bars are the positions of the Bragg peaks. The lower curve shows the difference between observed and calculated patterns. The dots and continuous line above the Bragg peak positions are the observed and calculated patterns, respectively.

Table 1
Experimental cell parameters of the Sr_2CeO_4 photoluminescent phase present in the S33 sample compared with the same phase reported by Danielson et al. [4].

Rietveld agreement indexes at the end of the refinements and unit cell dimensions		
	Values of this work	Reported by Danielson et al. [4]
a/Å	6.1174(1)	6.11987(9)
b/Å	10.3463(1)	10.3495(2)
c/Å	3.5965(0)	3.5970(1)
V/Å^3	227.63(1)	227.79(1)
c/a	0.5879	
R_{wp}	0.1460	**
S	1.47	**
R_F^2	0.0782	**

presence of different phases as impurities and may somehow affect the values of these energies. Thus, for a better understanding of this influence it is necessary to evaluate the amount of secondary phases present in each case and to correlate it with the spectroscopic properties presented by the produced phosphors.

Based on the recorded photoluminescent spectra (Figs. 1(A–C)), the relative emission intensity of the S10, S25 and S33 samples were compared and are depicted in Fig. 2 in graphic form. It is possible to verify that S33 shows the highest relative photoluminescence intensity, differently that results reported in the literature [27]. From the XRD patterns (Fig. 3), the phase evolution of the synthesized powder at different cerium concentrations can be observed and both the S25 and S33 samples display the higher percentage of the Sr_2CeO_4 phase (different relative intensity between phases). Therefore, due to the fact that S33 showed a higher relative emission intensity as well as a higher phosphor phase percentage, it was chosen to be evaluated by the Rietveld refinement in order to generate information about the amounts of all crystalline phases present in this material.

The Rietveld plot of the S33 sample pattern displaying the adjusted curve and the different phase percentages present in this phosphor are depicted in Fig. 4. The refined unit-cell parameters achieved by the Rietveld method for the photoluminescent Sr_2CeO_4 phase detected in the S33 sample are listed in Table 1. This table shows the estimated refinement indexes and unity cell dimensions of the obtained Sr_2CeO_4 phase compared with the same phase reported by Danielson et al. [4].

The quantitative phase analysis of the S33 sample (Fig. 4) revealed that the Sr_2CeO_4 phase is the primary component (53.1 wt%), whereas the impurity phases $SrCeO_3$ (38.6 wt%) and

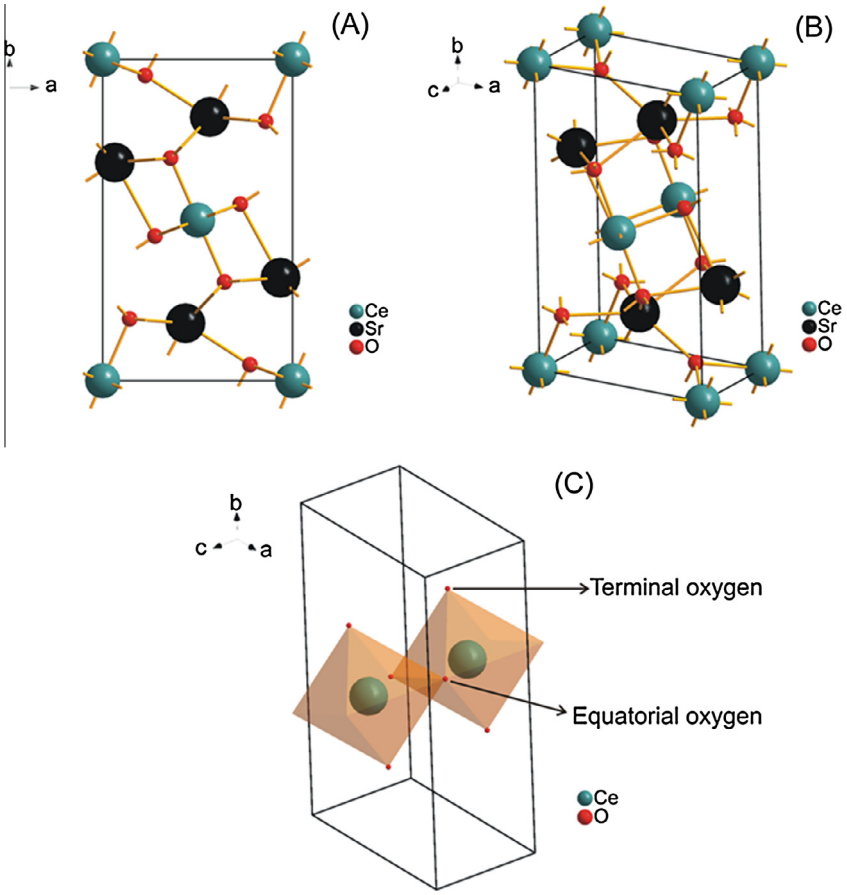

Fig. 5. Crystalline structure of Sr_2CeO_4: (A) visualization from direction *z*, (B) among different axis, and (C) octahedron structure showing different positions of O^{2-}.

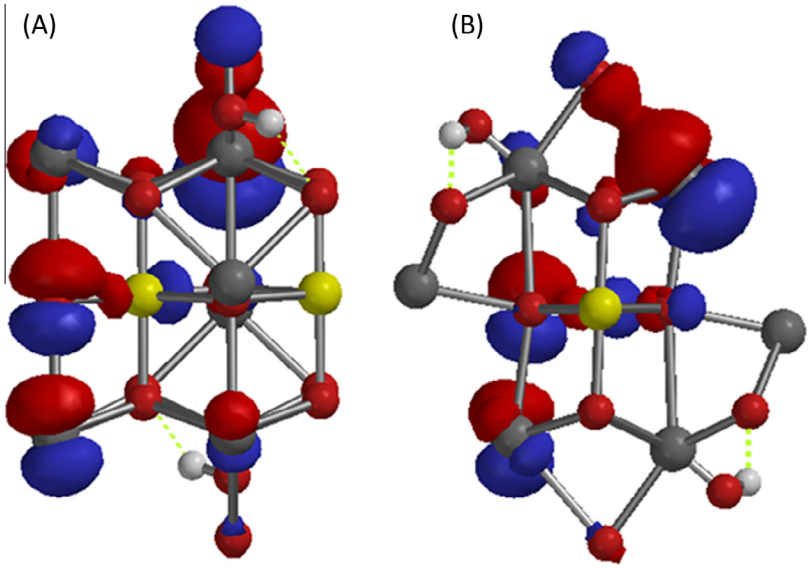

Fig. 6. Sparkle PM7 frontier orbitals (HOMO–LUMO) for Sr_2CeO_4 unit cell, in two views.

$SrCO_3$ (8.1 wt%) have lower concentrations as compared to other studies reported for bulk samples previously [4,12]. In those Refs. [4,12], the synthesis by using solid state method from $SrCO_3$ and CeO_2 precursors at 1000 °C during 12 h yielded about 62% $SrCO_3$, 24% $SrCeO_3$, 12% Sr_2CeO_4, and 4% CeO_2. Therefore, in the present work, it is important to emphasize that a large amount of Sr_2CeO_4 in a bulk form was successfully produced by the oxalate precursor, by using similar time and temperature conditions, yielding the photoluminescent phase at a 442 wt% greater quantity than that reported in those works [4,12].

According to Finger et al. [31], the photoluminescent Sr_2CeO_4 phase has an orthorhombic structure, and Chen et al. [17], Lee

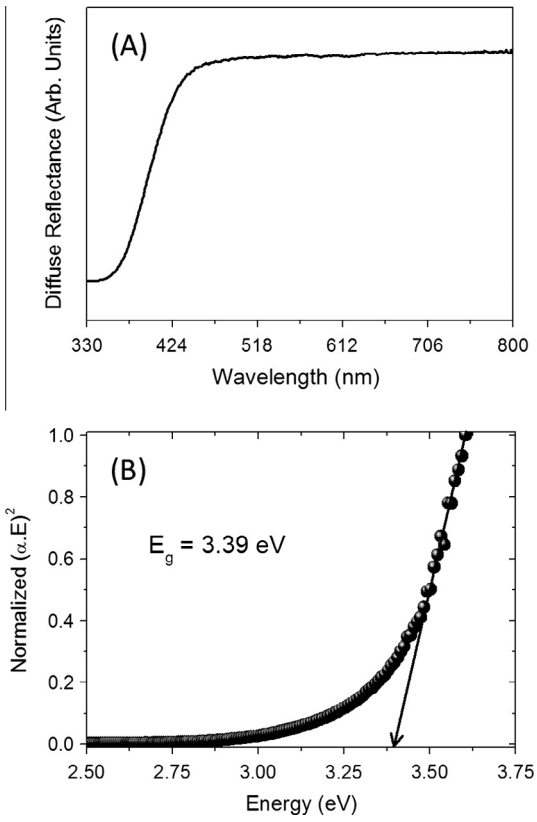

Fig. 7. (A) Diffuse reflectance spectrum of the S33 sample and (B) band-gap calculations based on the Kubelka–Munk equation.

et al. [34], and Yu et al. [9] have also published papers in agreement with such assignment. The Sr_2CeO_4 structure obtained by the Rietveld [5] refinement performed for S33 in different viewings is depicted in Fig. 5. In Fig. 5(A) it is possible to see the structure of the photoluminescent Sr_2CeO_4 phase from the *z*-axis, with excellent details about the position of the atoms within the unit cell. To facilitate viewing, Fig. 5(B) shows the same structure with visualization along the three axes (*x*, *y* and *z*). In addition, Fig. 5(C) shows the structure with the octahedron inside the cell, showing the exact position of the different oxygens responsible for the origin of the different emission band deconvoluted in the emission spectra.

Using the results obtained by the Rietveld refinement was possible to calculate the theoretical band gap value of the Sr_2CeO_4 photoluminescent phase. The energy gap values were calculated at semi empirical Sparkle/PM7 level of theory by solid state calculation. The main result showed that the band gap obtained from HOMO–LUMO, Fig. 6 orbitals was 3.4 eV. To compare the theoretical band gap values, reflectance diffuse spectrum was obtained, Fig. 7(A) and the band gap values based on the Kubelka–Munk, Fig. 7(B), equation was determined, and the value found was 3.39 eV. The results of the theoretical and experimental band-gap values are in good agreement when compared with the experimental one (3.39 eV) estimated from diffuse reflectance and Kubelka–Munk equations. These results emphasize the capability of the use of the Sparkle model for the prediction of physical chemical properties containing within the PM7 semi empirical model, as well as the usefulness of theoretical calculations for materials modeling. Based on the photoluminescence spectrum of the S33 sample (Fig. 1(A)), the CIE chromaticity diagram 1931 was obtained, and the result depicted in Fig. 8 helps us view exactly the color emitted by this photoluminescent material acquired by the synthesis reported here.

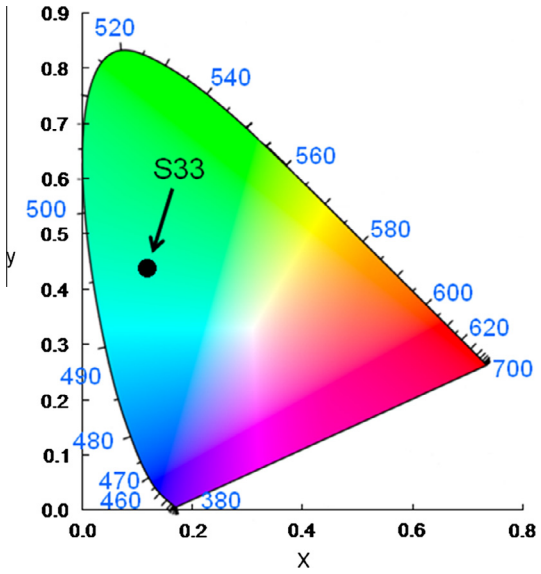

Fig. 8. CIE chromaticity diagram 1931 for S33 sample based on the photoluminescence spectra (Fig. 1(C)).

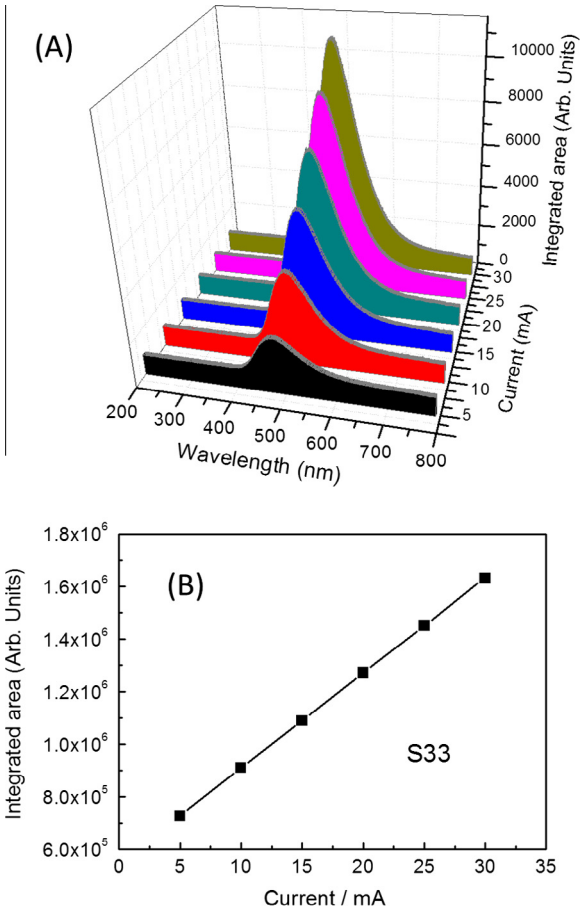

Fig. 9. (A) Emission spectra under X-ray excitation and (B) linear fit of the integrated area of the band of the emission spectra.

The S33 material was excited using X-rays, with different current values. The results are shown in Fig. 9(A). As can be seen, the material showed intense emission with the maximum around 475 nm. The emission intensity increased linearly Fig. 9(B) as a function of current used as excitation source.

4. Conclusion

The oxalate precursor used to prepare the photoluminescent compound discussed in this work appears to be feasible to produce phosphors with interesting optical properties in powder form. Despite some undesirable phases, such as $SrCeO_3$ and $SrCO_3$, have also been obtained together with the photoluminescent Sr_2CeO_4 phase, an intense photoluminescence emission was observed with naked eyes. Based on the results acquired from the Rietveld refinement of the Sr_2CeO_4 crystalline structure, as well as many papers reported in the literature, it was possible to understand with detail the position of Ce(IV) and O^{2-} and, consequently, the source of the photoluminescence of this material. The presence of $SrCeO_3$ and $SrCO_3$ phases somehow affects the energy of the deconvoluted bands in the emission spectra. The theoretical and experimental band gap values obtained are very in accordance. From the CIE chromaticity diagram 1931 applied for the S33 sample, it was observed that its emission color is in accordance with the behavior demonstrated by this photoluminescent material. Based on the results reported here, for this synthesis, we confirmed that the 33 mol% Ce(III)-doped strontium oxalate precursors is the optimum amount of this ion to obtain adequate photoluminescence properties. Thus, this compound can be used in the manufacturing of devices that need materials with intense emission. The emission spectrum under excitation with X-ray shows that this material shows intense emission around 475 nm. This material is also a good candidate for use as a scintillator or in the improvement of efficiency of solar cells, when excited in the UV–vis region. Future work will study and improve the optical quality of this material.

Acknowledgements

The authors would like to thank FAPEMIG, FAPESP and CNPq for the financial support and Jennifer Esbenshade for English revisions. This work is a collaboration research project of members of the Rede Mineira de Química (RQ-MG) supported by FAPEMIG (Project. REDE-113/10).

References

[1] G. Blasse, A. Bril, The absortion and emission spectra of some important activators, Philips Tech. Rev. 31 (1970) 304.
[2] P. Braterman, G. Blasse, A. Müller, E. Baran, R. Carter, The influence of charge-transfer and rydberg states on the luminescence properties of lanthanides and actinides, Spectra and Chemical Interactions, Springer Berlin/Heidelberg 26 (1976) 43–79.
[3] G. Blasse, B.C. Grabmaier, Luminescent Materials, Springer-Verlag, Berlin/Heidelberg, 1994.
[4] E. Danielson, M. Devenney, D.M. Giaquinta, J.H. Golden, R.G. Haushalter, E.W. McFarland, D.M. Poojary, C.M. Reaves, W.H. Weinberg, X. Di Wu, X-ray powder structure of Sr_2CeO_4: a new luminescent material discovered by combinatorial chemistry, J. Mol. Struct. 470 (1998) 229–235.
[5] H. Rietveld, A profile refinement method for nuclear and magnetic structures, J. Appl. Crystallogr. 2 (1969) 65–71.
[6] Y. Zhai, X. Zhou, G. Yang, Y. Meng, S. Yao, Z. Guo, Synthesis and luminescent properties of superfine Sr_2CeO_4 phosphors by Sol–Gel auto-combustion method, J. Rare Earth 24 (2006) 281–284.
[7] L. Li, S. Zhou, S. Zhang, Investigation on charge transfer bands of Ce^{4+} in Sr_2CeO_4 blue phosphor, Chem. Phys. Lett. 453 (2008) 283–289.
[8] P.N. Yocum, Rekindled interest in electroluminescent displays for commercial uses, The Electrochem. Soc. Interf. 3 (1994) 36–38.
[9] X. Yu, X. He, S. Yang, X. Yang, X. Xu, Synthesis and luminescence of Sr_2CeO_4 superfine particles by citrate–gel method, Mater. Lett. 58 (2004) 48–50.
[10] C.X. Zhang, J.S. Shi, X.J. Yang, L.D. Lu, X. Wang, Preparation, characterization and luminescence of Sm^{3+} or Eu^{3+} doped Sr_2CeO_4 by a modified sol–gel method, J. Rare Earth 28 (2010) 513–518.
[11] C.H. Lu, T.Y. Wu, C.H. Hsu, Synthesis and photoluminescent characteristics of Sr_2CeO_4 phosphors prepared via a microwave-assisted solvothermal process, J. Lumin. 130 (2010) 737–742.
[12] E. Danielson, M. Devenney, D.M. Giaquinta, J.H. Golden, R.C. Haushalter, E.W. McFarland, D.M. Poojary, C.M. Reaves, W.H. Weinberg, X.D. Wu, A rare-earth phosphor containing one-dimensional chains identified through combinatorial methods, Science 279 (1998) 837–839.
[13] C. Zhang, W. Jiang, X. Yang, Q. Han, Q. Hao, X. Wang, Synthesis and luminescent property of Sr_2CeO_4 phosphor via EDTA-complexing process, J. Alloys Comp. 474 (2009) 287–291.
[14] X. Liu, Y. Luo, J. Lin, Synthesis and characterization of spherical Sr_2CeO_4 phosphors by spray pyrolysis for field emission displays, J. Cryst. Growth 290 (2006) 266–271.
[15] L. Van Pieterson, S. Soverna, A. Meijerink, On the nature of the luminescence of Sr_2CeO_4, J. Electrochem. Soc. 147 (2000) 4688–4691.
[16] D. Xing, M. Gong, X. Qiu, D. Yang, K.W. Cheah, Characterization of superfine sr_2ceo_4 powder prepared by microemulsion–heating method, J. Rare Earth 24 (2006) 289–293.
[17] S.J. Chen, X.T. Chen, Z. Yu, J.M. Hong, Z. Xue, X.Z. You, Preparation and characterization of fine Sr_2CeO_4 blue phosphor powders, Solid State Commun. 130 (2004) 281–285.
[18] Y.B. Khollam, S.B. Deshpande, P.K. Khanna, P.A. Joy, H.S. Potdar, Microwave-accelerated hydrothermal synthesis of blue white phosphor: Sr_2CeO_4, Mater. Lett. 58 (2004) 2521–2524.
[19] Y.D. Jiang, F. Zhang, C.J. Summers, Z.L. Wang, Synthesis and properties of Sr_2CeO_4 blue emission powder phosphor for field emission displays, Appl. Phys. Lett. 74 (1999) 1677–1679.
[20] T. Masui, T. Chiga, N. Imanaka, G.Y. Adachi, Synthesis and luminescence of Sr_2CeO_4 fine particles, Mater. Res. Bull. 17 (2003) 17–24.
[21] Y. Tang, H. Guo, Q. Qin, Photoluminescence of Sr_2CeO_4 phosphors prepared by microwave calcination and pulsed laser deposition, Solid State Commun. 121 (2002) 351–356.
[22] O.A. Serra, V.P. Severino, P.S. Calefi, S.A. Cicillini, The blue phosphor Sr_2CeO_4 synthesized by Pechini's method, J. Alloys Comp. 323–324 (2001) 667–669.
[23] H.E. Hoefdraad, Charge-transfer spectra of tetravalent lanthanide ions in oxides, J. Inorg. Nucl. Chem. 37 (1975) 1917–1921.
[24] J. Gomes, A.M. Pires, O.A. Serra, Morphological study of Sr_2CeO_4 blue phosphor with fine particles, Quim. Nova 27 (2004) 706–708.
[25] J.L. Ferrari, A.M. Pires, M.R. Davolos, C.A. Ribeiro, Thermal decomposition studies of Cerium(III)-doped strontium oxalate as luminescent material precursor, Eclet. Quim. 37 (2002) 315–328.
[26] C.H. Lu, C.-T.J. Chen, Luminescent characteristics and microstructures of Sr_2CeO_4; phosphors prepared via sol–gel and solid-state reaction routes, J. Sol–Gel Sci. Technol. 43 (2007) 179–185.
[27] J.L. Ferrari, A.M. Pires, A.O. Serra, M.R. Davolos, Luminescent and morphological study of Sr_2CeO_4 blue phosphor prepared from oxalate precursors, J. Lumin. 131 (2011) 25–29.
[28] A.C. Larson, R.B. Von Dreele, General Structure Analysis System (GSAS), Los Alamos National Laboratory Report LAUR 1 (2004) 86–748.
[29] B.H. Toby, EXPGUI – A graphical user interface for GSAS, J. Appl. Crystallogr. 34 (2001) 210–213.
[30] R.A. Young, P. Desai, Crystallite size and microstrain indicators in Rietveld Refinement, Archiwum Nauki o Materialach. 10 (1989) 71–90.
[31] L.W. Finger, D.E. Cox, A.P. Jephcoat, A correction for powder diffraction peak asymmetry due to axial divergence, J. Appl. Crystallogr. 27 (1994) 892–900.
[32] M.A. Cebim, H.H.S. Oliveira, N. Barelli, M.R. Davolos, Quim. Nova 34 (2011) 1057–1062.
[33] S.S. Moosath, J. Abraham, T.V. Swaminathan, Thermal decomposition of rare earth metal oxalates: IV. Oxalates of cerium and thorium, Z. F. Anorg. Allg. Chem. 324 (1963) 103–105.
[34] Y.E. Lee, D.P. Norton, J.D. Budai, P.D. Rack, M.D. Potter, Photo and cathodoluminescence characteristics of blue-light-emitting epitaxial Sr_2CeO_4 thin-film phosphors, Appl. Phys. Lett. 77 (2000) 678–680.